

## Appendix A: Resonant elements

For all bodies inside the 3:2 mean-motion resonance with Jupiter, we also computed synthetic resonant elements, by means of a numerical integration of their orbits. We used the symplectic integrator SWIFT (Levison & Duncan 1994), specifically the method MVS2 (Laskar & Robutel 2001). Our dynamical model included gravity of the Sun and four massive planets (Jupiter to Neptune). We applied the barycentric correction and the rotation to invariant plane. No non-gravitational effects were used.

Osculating elements were sampled at 1 y intervals. Mean elements were computed by digital filtering (Quinn et al. 1991), in order to suppress short-period oscillations unrelated to librations. We applied the filter ‘A’ with a decimation factor of 10; the intermediate time step was thus 10 y.

Resonant elements (Ferraz-Mello et al. 1998; Brož & Vokrouhlický 2008; Brož et al. 2011) were defined by the critical angle of the 3:2 mean-motion resonance with Jupiter

$$\sigma = 3\lambda' - 2\lambda - \varpi, \quad (\text{A.1})$$

where  $\lambda'$  is the true longitude of Jupiter,  $\lambda$ , the true longitude of asteroid,  $\varpi$ , the pericentre longitude of asteroid. For bodies inside a resonance,  $\sigma$  librates around  $0^\circ$ , while the semimajor axis  $a$  and the eccentricity  $e$  exhibit coupled oscillations. We used an approximate surface of section

$$|\sigma| < 10^\circ \wedge \dot{\sigma} > 0 \wedge |\varpi - \varpi'| < 10^\circ \quad (\text{A.2})$$

and monitored the corresponding mean elements within a window 0.01 My wide. The tolerance of  $10^\circ$  assured that the criterion was fulfilled at least once. The second intermediate time step was 0.01 My.

Finally, we performed averaging of any remaining oscillations, related to secular perturbations by Jupiter, perturbations by other planets, chaotic motion due to overlapping resonances etc. We used a window 10 My and the output time step was 10 My. These elements  $a_r$ ,  $e_r$ ,  $I_r$  are approximate integrals of motion. Their uncertainties were estimated from a continuation of the integration up to 20 My. The medians of differences were  $\Delta a = 7 \times 10^{-5}$  au,  $\Delta e = 9 \times 10^{-5}$ ,  $\Delta I = 0.004^\circ$ , respectively. This is certainly sufficient for an identification of families.

## Appendix B: Family identification

To identify the families, we used recent catalogues (Jul 2024), namely Astorb (Moskovitz et al. 2019), Wise (Nugent et al. 2015), Akari (Usui et al. 2011), and Sloan DSS (Parker et al. 2008). We combined both orbital data and physical data, in order to obtain a complete characterisation.

The identification procedure consisted in the hierarchical clustering method (HCM; Zappalà et al. 1995) with the cut-off velocity adjusted separately for each family (cf. (Nesvorný et al. 2015)). Additionally, we performed a removal of interlopers based on the eccentricity vs. absolute magnitude criterion

$$H > 5 \log_{10} \left( \frac{|e - e_0|}{C} \right), \quad (\text{B.1})$$

because inside a 1-st-order resonance, the Yarkovsky effect leads to a drift in eccentricity, not in semimajor axis (Brož & Vokrouhlický 2008). The Hilda and Potomac families were separated by a  $\sin I = 0.175$ ; otherwise they would merge together.

The list of all families is in Tab. B.1. Four new ones were found, namely Francette, Potomac, Guinevere, and (269345). Their positions are shown in Fig. B.1, and individually also in

**Table B.1.** List of asteroid families found inside the 3:2 resonance with Jupiter.

| number  | designation | $v_{\text{cut}}$<br>m s <sup>-1</sup> | $N$  | notes   |
|---------|-------------|---------------------------------------|------|---------|
| 153     | Hilda       | 90                                    | 1066 | C-type  |
| 1911    | Schubart    | 60                                    | 1882 | C-type  |
| 1212*   | Francette   | 30                                    | 151  |         |
| 1345*   | Potomac     | 140                                   | 506  | diffuse |
| 2483*   | Guinevere   | 40                                    | 54   |         |
| 269345* | 2008 TG106  | 54                                    | 17   | tiny    |

**Notes.**  $v_{\text{cut}}$  is the cutoff velocity,  $N$ , the number of family members, \* denotes a new family.

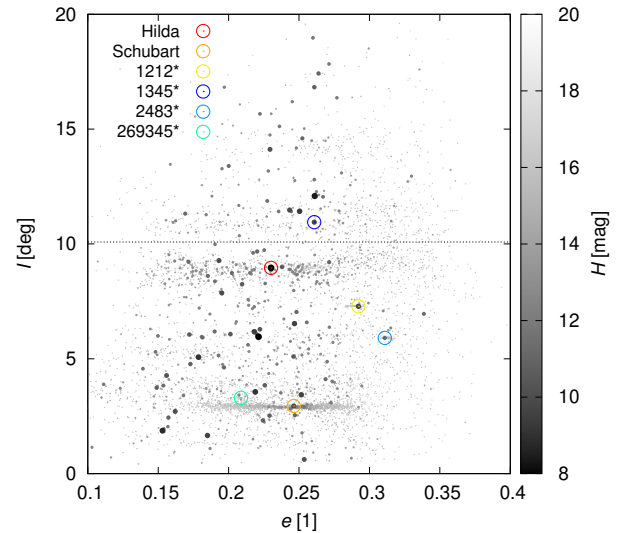


**Fig. B.1.** Synthetic resonant elements of asteroids in the 3:2 resonance with Jupiter. The resonant eccentricity  $e_r$  vs. inclination  $I_r$  is plotted. The sizes of symbols are inversely proportional the absolute magnitude  $H$ . Both known and new families are indicated by coloured circles, at the positions of asteroids (153) Hilda, (1911) Schubart, (1212) Francette, (1345) Potomac, (2483) Guinevere, and (269345) 2008 TG106.

Fig. B.2. The Potomac family is diffuse, its spatial density is about twice higher than that of background. This implies that some 50% fraction of the members should belong to the background population. The (269345) family is tiny, with only 17 members, but still statistically significant. All sizable families (except (269345)) do contribute to the overall distribution of orbital elements  $a_r$ ,  $e_r$ ,  $I_r$  and should be treated separately during debiasing of the population(s).

## References

- Brož, M., Vokrouhlický, D., Morbidelli, A., Nesvorný, D., & Bottke, W. F. 2011, MNRAS, 414, 2716
- Brož, M. & Vokrouhlický, D. 2008, MNRAS, 390, 715
- Ferraz-Mello, S., Michtchenko, T. A., & Roig, F. 1998, AJ, 116, 1491
- Laskar, J. & Robutel, P. 2001, Celestial Mechanics and Dynamical Astronomy, 80, 39
- Levison, H. F. & Duncan, M. J. 1994, Icarus, 108, 18
- Moskovitz, N., Schottland, R., Burt, B., et al. 2019, in EPSC-DPS Joint Meeting 2019, Vol. 2019, EPSC-DPS2019-644
- Nesvorný, D., Brož, M., & Carruba, V. 2015, Identification and Dynamical Properties of Asteroid Families, ed. P. Michel, F. E. DeMeo, & W. F. Bottke (Univ. Arizona Press), 297–321
- Nugent, C. R., Mainzer, A., Masiero, J., et al. 2015, ApJ, 814, 117
- Parker, A., Ivezić, Ž., Jurić, M., et al. 2008, Icarus, 198, 138

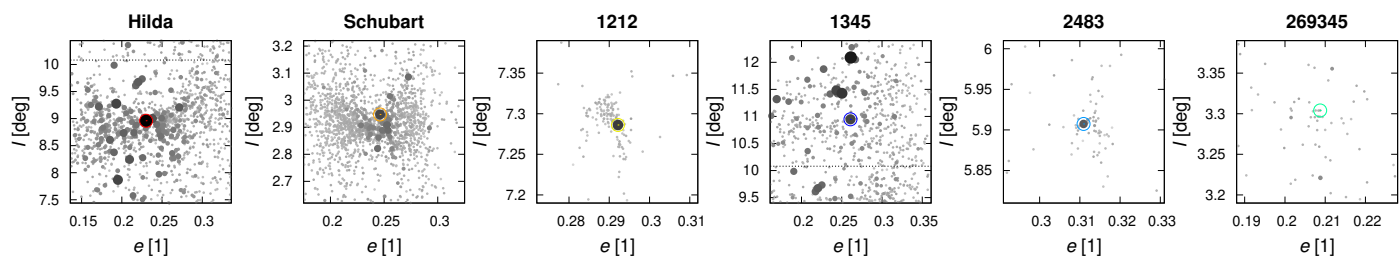


**Fig. B.2.** Same as Fig. B.1, but for individual families.

Quinn, T. R., Tremaine, S., & Duncan, M. 1991, AJ, 101, 2287

Usui, F., Kuroda, D., Müller, T. G., et al. 2011, PASJ, 63, 1117

Zappalà, V., Bendjoya, P., Cellino, A., Farinella, P., & Froeschlé, C. 1995, Icarus, 116, 291